

The Reaction Rate Constant of Chlorine Nitrate Hydrolysis

Thomas Loerting and Klaus R. Liedl*^[a]

Abstract: The first-order rate constant for the decomposition of chlorine nitrate (ClONO₂) by water in a cyclic 1:3 complex at stratospheric temperatures is shown to be close to the values for the hydrolysis rate coefficient of chlorine nitrate on an ice surface determined in the laboratory. On the other hand the rate constants calculated for the cyclic 1:1 and 1:2 complexes are much lower than the experimental results. From the

mechanistic point of view the reaction is found to be similar to a S_N2 mechanism and coupled with water-mediated proton transfer in accordance with the intriguing findings of Bianco and Hynes [R. Bianco, J. T. Hynes, *J. Phys. Chem. A*

1998, 102, 309–314]. The function of additional water molecules is to act as a catalyst, that is, to accelerate the hydrolysis process. Quantum-mechanical tunneling is negligible above 125 K in the 1:3 complex and above 175 K in the 1:2 complex. At temperatures below these limits all involved protons tunnel through the barrier at energies at least 5 kcal mol⁻¹ below the barrier-top in a concerted, but asynchronous manner.

Keywords: ab initio calculations • hydrolysis • hydrogen transfer • kinetics • ozone depletion

Introduction

The “ozone hole” was recognized for the first time in 1985 above Antarctica,^[1] and this recognition has resulted in a wealth of studies on the chemical reactions and physical mechanisms involved in ozone depletion and rebuilding.^[2–6] At Northern hemisphere midlatitudes the decline in the vertical profile of ozone amounts to about 7% per decade (at both 15 km and 40 km altitude).^[7] At the poles much more tremendous depletions could be observed. Record low levels of column ozone (down to a 100% depletion in the 1990s) can be observed annually in spring at a height of about 10–20 km.^[8] The enormous depletions above Antarctica and Arctica at these altitudes can directly be correlated with the occurrence of polar stratospheric clouds (PSC).^[9, 10] This relation has been attributed to heterogeneous processes taking place on the cloud surface listed in Equations (1) and (2).



After desorption from the cloud Cl₂ and HOCl are photolyzed in spring by sunlight to produce chlorine radicals (Cl•, ClO•)

actively converting ozone (O₃) to molecular oxygen (O₂).^[11–14] While HNO₃ is incorporated in the particles at about 200 K the chlorine compounds are not,^[12] which has the effect that the amount of radical recombination, for example, by Equation (3), is reduced and the total concentration of ozone-depleting radicals is increased.



Because of this relevance to ozone depletion many researchers have designed experiments to understand chlorine nitrate chemistry. About 15 years ago upper limits for the rate constant of the homogeneous gas-phase reaction have been determined and shown to be much too low to be important in the context of ozone depletion,^[11, 14] which explains why reduced ozone levels can be found mainly above the poles. After this discovery numerous laboratory experiments have focussed on determining the reaction probabilities γ for chlorine nitrate hydrolysis on different surfaces believed to mimic PSCs^[9, 15–17] at temperatures between 140 K and 200 K including ice, sulfuric acid solutions or nitric acid trihydrate.^[18–23] A common conclusion arising as a result to these experiments is the sensitivity of γ on equilibrium water vapour pressures, which are lowest for surfaces coated with acids such as nitric acid trihydrate. It was found that water in condensed phases is required to measure reaction probabilities high enough to be able to explain ozone depletion. These fascinating results have attracted theoretical chemists to seek answers on the molecular mechanism and the role of water in such heterogeneous processes.^[24–29] With the use of small gas-phase clusters made of ClONO₂ and H₂O first the binding-site

[a] Prof. Dr. K. R. Liedl, Dr. T. Loerting
Institute of General, Inorganic and Theoretical Chemistry
University of Innsbruck, Innrain 52a, 6020 Innsbruck (Austria)
Fax: (+43) 512-507-5144
E-mail: klaus.liedl@uibk.ac.at

of water^[24] and second a mechanism involving a S_N2 -type attack of water on the Cl–ONO₂ bond that is favoured by a concerted proton transfer (PT) generating a stronger, hydroxyl-like, nucleophile^[25, 26] could be deduced. These results are perfectly consistent with ¹⁸O-substitution experiments.^[30] Furthermore mass spectroscopic and infrared studies indicated this change in the degree of polarization of this bond leading to enhanced electrophilicity of the chlorine atom.^[31, 32] The reaction barrier was shown to be very high in an 1:1 complex and to be reduced subsequently on the addition of water molecules (both by water molecules directly reacting in the ring and by water molecules acting just as microsolvant).^[29] The decomposition in an 1:6 complex of chlorine nitrate with water was found to be essentially barrierless.^[27, 28]

In order to reveal details about the reaction mechanism and to be able to convert bare barrier heights to valuable reaction rate constant information, the reaction path has to be generated step by step. The additional calculation of zero-point energies along this path allows quantum effects such as tunneling to be incorporated in the pre-exponential factor of the Arrhenius rate equation. To allow corner-cutting and tunneling on the concave side of the reaction path, the potential energy has to be calculated in the wide region called reaction swath as well. In this work we have calculated approximately 1000 points on the reaction surface for the conversion of ClONO₂ to HOCl and HNO₃ on each of the hypersurfaces for the 1:1, 1:2 and 1:3 clusters of chlorine nitrate and water by hybrid density functional theory. We focus our attention on Equation (1), which has been found to be important especially at water-rich conditions.^[13, 14, 33] The competing decomposition of ClONO₂ by HCl [Eq. (2)] on ice surfaces was investigated separately with the same method and will be presented on its own.^[34] Highly accurate ab initio methods taking electron correlation carefully into account were used to evaluate the reaction barrier as accurately as

possible. These calculations do not employ empirical potentials at all and, for the first time, provide the opportunity to compare reaction rates of model substances with experimentally determined reaction probabilities of chlorine nitrate on ice surfaces. Furtheron, it is possible to judge to which extent and at which temperatures proton tunneling is important in such reaction systems.

Methods

Stationary points: Geometry optimization of the equilibrium structures and the transition states was performed both by hybrid density functional theory (B3LYP/6-31+G(d))^[35, 36] and second-order perturbation theory (MP2/aug-cc-pVDZ)^[37] as implemented in Gaussian98.^[38] The nature of these stationary points was verified by calculating vibrational frequencies. The Hessian matrix contains positive eigenvalues only for minima and exactly one negative eigenvalue for transition states. Predictions of reaction dynamics critically depend on the reaction barrier, that is, the difference in electronic energy between transition state and minima, and the tunneling correction factor. The importance of the latter vanishes when the temperature is higher than the first crossover-temperature.^[39] In the case of the “impure” proton transfer investigated herein, that is, a proton transfer that is accompanied by heavy atom motion, both crossover-temperatures are lower than in the case of pure proton transfer exhibiting a reduced mass near unity. Therefore, the tunneling correction factors were expected to be a priori rather low for chlorine nitrate hydrolysis involving substantial movement of the chlorine atom. For that reason the importance of an accurate reaction barrier is even more crucial for the reactions investigated. We employed single-point energy calculations at the CCSD(T)/aug-cc-pVDZ//MP2/aug-cc-pVDZ^[40] level of theory and by Gaussian-2 theory using MP2 (G2(MP2))^[41] to reach a reasonable accuracy of the barrier height.

Ab initio reaction path and rate constants: Starting from the transition state the reaction path was generated as the steepest descent path in mass-scaled coordinates employing a scaling mass of 1 amu throughout. This path, called minimum energy path (MEP) or intrinsic reaction coordinate (IRC), was generated by using the Page–McIver algorithm^[42] employing a step size of 0.05 Bohr (1 Bohr corresponds to 0.53 Å). The distance of a point on the potential energy surface to the transition state is denoted s and given a “+” sign if on the product side and a “–” sign if on the reactant side. Vibrational frequencies and partition functions were calculated every third point on the hypersurface. On both branches of the reaction coordinate the path was stopped when stable minima structures were reached, that is, when the gradient vanished. This required altogether about 400 points and was done using hybrid density functional theory (B3LYP/6-31+G(d)), which was designed to incorporate electron correlation at a cost comparable to Hartree–Fock calculations, which do not incorporate electron correlation effects. The use of such a procedure was found to be successful for

Abstract in German: Die berechnete Geschwindigkeitskonstante der Zersetzung von Chlornitrat (ClONO₂) durch Wasser in einem ringförmigen 1:3 Komplex bei stratosphärischen Temperaturen liegt sehr nahe bei der im Labor bestimmten Geschwindigkeitskonstante für die Hydrolyse von Chlornitrat auf einer Eisoberfläche. Die vorhergesagten Geschwindigkeitskonstanten für die ringförmigen 1:1 und 1:2 Komplexe sind hingegen deutlich niedriger als die experimentellen Ergebnisse. Von der mechanistischen Seite betrachtet verläuft die Reaktion S_N2 -artig und ist gekoppelt mit wasserunterstütztem Protonentransfer. Dies ist im Einklang mit den faszinierenden Erkenntnissen von Bianco und Hynes (R. Bianco, J. T. Hynes, *J. Phys. Chem. A* **1998**, *102*, 309–314). Die zusätzlichen Wassermoleküle üben die Funktion eines Katalysators aus, das heißt sie beschleunigen den Hydrolyseprozess. Quantenmechanisches Tunneln ist oberhalb von 125 K im 1:3 Komplex, sowie oberhalb von 175 K im 1:2 Komplex vernachlässigbar. Bei Temperaturen unterhalb dieser Grenzen tunneln alle beteiligten Protonen gleichzeitig, aber asynchron durch die Reaktionsbarriere, und zwar bei Energien von mindestens 5 kcal mol⁻¹ unterhalb des Gipfels der Barriere.

“pure” proton transfer reactions, which are more difficult to be described in terms of quantum tunneling.^[43–45]

From these data reaction rate constants were obtained by applying canonical variational transition state theory (CVTST)^[46, 47] according to the techniques implemented in Polyrate8.2.^[48, 49] We employed a highly sophisticated dual-level direct dynamics procedure, which is based on the combination of two potential energy surfaces for the same reaction system by a logarithmic interpolation procedure (ICL).^[50–53] That is, the reaction path and especially the reaction barrier obtained from hybrid density functional theory were adjusted from (lower level) B3LYP/6-31+G(d) to (higher level) G2(MP2) results.

Quantum mechanical tunneling and corner cutting: The tunneling correction factor was calculated according to the microcanonical optimized multidimensional tunneling model and by allowing tunneling into all available vibrationally excited states.^[54–57] This scheme allows the reaction system to take reaction paths different from the MEP, which are shorter, but more demanding in terms of energy. This is called multidimensional corner cutting. Such paths may be favoured compared with the MEP, as they involve shorter paths and are, therefore, accelerated by quantum mechanical tunneling. As this task is computationally very expensive the maximum of the approximative small (SCT)^[58, 59] and large curvature tunneling (LCT)^[60–63] correction is taken. Specifically, the centrifugal-dominant small curvature semiclassical adiabatic ground state (CD-SCSAG) and the large curvature ground state approximation, version 3 (LCG3) methods were used to calculate SCT and LCT corrections, respectively. We were able to cope with this task by calculating an additional grid of 600 points in the reaction swath, that is, the region on the concave side of the reaction path extending beyond the transverse vibrational turning points and/or beyond the local radius of curvature.^[54, 57, 62, 63] The LCG3 scheme tends to result in tunneling correction factors slightly too high, as it does not treat anharmonicity effects along low-energy corner-cutting tunneling paths properly. Unfortunately the very latest LCG scheme (LCG4)^[64] was not available to us at the time of the calculations. However, it turned out that the SCT tunneling corrections are larger than the LCT tunneling corrections for the investigated reactions down to low temperatures of about 150 K, so that the use of LCG3 instead of LCG4 does not pose a problem in the case of chlorine nitrate hydrolysis at stratospheric temperatures (> 180 K).

Results

Stationary structures: The optimized structures involving up to three water molecules can be seen in Figure 1. Similar chlorine nitrate–water systems have been investigated previously by other groups. Ying and Zhao did prove that the best binding site for water involves interaction between the water oxygen and the chlorine atom,^[24] which is also found in this work. Bianco and Hynes,^[25, 26] McNamara and Hillier,^[27, 28] as well as Xu and Zhao^[29] systematically studied the decomposition reaction involving a different number of micro-

solvating water molecules up to eight water molecules. A general consensus is that the reaction barrier to chlorine nitrate decomposition vanishes on increasing the number of water molecules. Up to about six water molecules the reaction was shown to be completely nonionic. All minima investigated here do not show ionic character as well, as can be seen in Figure 1. Above six water molecules, ions such as H_2OCl^+ or H_3O^+ and NO_3^- were found to be stable intermediates and

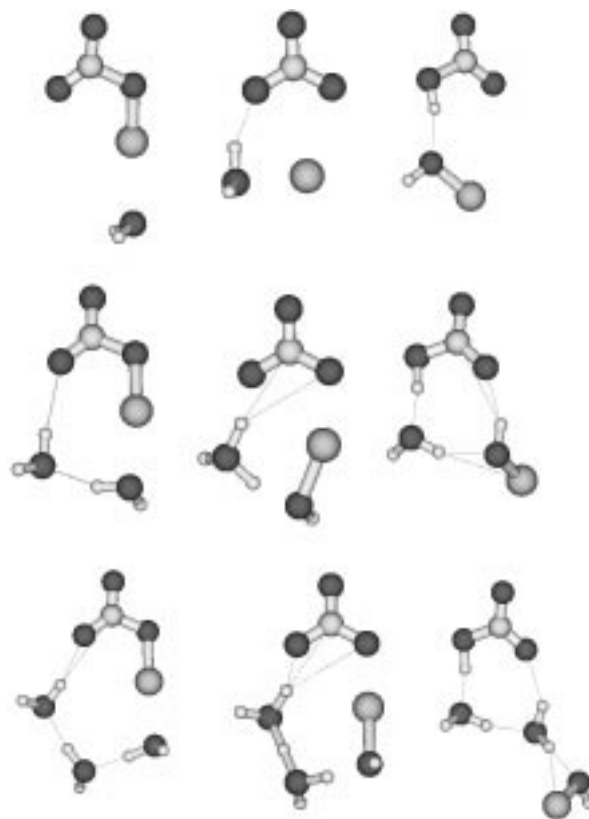


Figure 1. Stationary structures involved in the hydrolysis of chlorine nitrate in the presence of one (top), two (middle) and three (bottom) water molecules as found at B3LYP/6-31+G(d) level of theory.

the barrier to decomposition was found to be close to zero.^[27, 28] These species are discussed in context of the so-called “ion-catalyzed water mechanism” in the literature.^[27, 65, 66] From our calculations electron correlation effects favour product geometries, in which the chlorine atom is found outside the reactive ring when comparing to the Hartree–Fock calculations of Xu and Zhao.^[29] In case of two hydrolyzing water molecules (cf. Figure 1, $n=2$) the HOCl moiety rotates, so that the hydroxyl group takes the role of the chlorine atom. In the case of three hydrolyzing water molecules ($n=3$) the HOCl moiety moves out of the ring completely in order to produce $\text{HNO}_3 \cdot 2\text{H}_2\text{O}$, which is more stable than $\text{HNO}_3 \cdot \text{HOCl} \cdot 2\text{H}_2\text{O}$.

Reaction energetics: The reaction barrier to decomposition is shown in Figure 2 and Table 1. The first striking feature is the enormous barrier, both in height and width, of the decomposition involving one molecule of water. Looking at the corresponding geometries in Figure 1 reveals that the rather

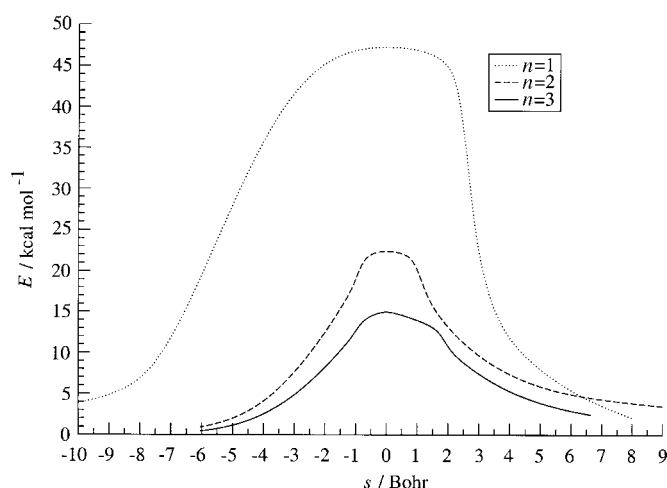


Figure 2. Energy along the classical reaction coordinate (MEP, IRC) as found at B3LYP/6-31+G(d) level of theory for the reaction $\text{ClONO}_2 \cdot n\text{H}_2\text{O} \rightarrow \text{HOCl} \cdot \text{HNO}_3 \cdot (n-1)\text{H}_2\text{O}$.

large $\text{OCl} \cdots \text{O}$ distance of 4.29 (4.44) Å at B3LYP/6-31+G(d) (MP2/aug-cc-pVDZ) level of theory prohibits the formation of a hydrogen bond between water and chlorine nitrate. Both hydrogen atoms of the water molecule are out of the plane built by the atoms of chlorine nitrate. Introducing a second water molecule fulfills a bifunctional role. On the one hand this water molecule acts as hydrogen-bond donor to an oxygen atom of chlorine nitrate, and on the other hand it acts as hydrogen-bond acceptor for a hydrogen bond with the first water molecule. One hydrogen atom of the first water molecule is forced, therefore, into the chlorine nitrate plane. As a result of the “closure” of the reactive ring by the second water molecule the barrier drops by about 32 kcal mol⁻¹ according to the electronic structure methods taking electron correlation most carefully into account, namely CCSD(T)/aug-cc-pVDZ and G2(MP2). Introducing a third water molecule in the reactive ring relieves steric strain. All hydrogen bonds are as short as 2.6–2.8 Å and rather linear, that is, between 166 and 177°, for the 1:3 complex of chlorine nitrate and water, whereas hydrogen bond distances of up to 3.3 Å and unfavourable O-H-O angles as low as 138° are

observed in the 1:1 and 1:2 complexes. This is quite unexpected, as a large ring containing seven heavy atoms and three hydrogen atoms is formed. For cycloalkanes the six-membered ring is the most stable one, which led Akhmat-skaya et al.^[67] to the statement that in the case of one participating water molecule “the transition state involves a six-membered ring, with presumably small strain, which suggests that inclusion of a further quantum mechanical water molecule would not greatly facilitate the reaction”.

As shown in Table 1 the electronic description for the $\text{ClONO}_2 \cdot 1\text{H}_2\text{O}$ system is rather difficult. Methods taking into account electron correlation in different manners lead to barriers varying between 47 and 63 kcal mol⁻¹. MP2 calculations with smaller basis sets at Hartree–Fock geometries yielded even barrier heights near 70 kcal mol⁻¹.^[29] However, two approaches to the reaction barrier taking electron correlation effects carefully into account, namely the G2(MP2) and CCSD(T)/aug-cc-pVDZ//MP2/aug-cc-pVDZ approaches, led to very similar “best estimates” of the reaction barrier of 58–59 kcal mol⁻¹. Comparing the results obtained from different electronic structure methods it can be seen that hybrid density functional theory underestimates the reaction barriers, especially because the $\text{OCl} \cdots \text{O}$ distance is underestimated by about 0.15 Å in the minima, but overestimated by 0.05 Å in the transition states, when comparing to MP2/aug-cc-pVDZ geometries. This underestimation was found to be rather typical for B3LYP in a database of 20 well-known reactions.^[68] Nevertheless, B3LYP/6-31+G(d) was used for the generation of the minimum energy path, as it is by far the cheapest method among the methods listed in Table 1 for the calculation of electronic properties. In order to account for the discrepancies in the reaction barrier, the hypersurface was interpolated to G2(MP2) barriers.^[53] When the number of water molecules is increased the difficulties in the electronic description decrease. G2(MP2) and CCSD(T) calculations yield very similar reaction barriers of about 26.5 kcal mol⁻¹ ($n=2$). Using the smaller 6-31+G(d) basis-set yields deviations of more than 3 kcal mol⁻¹ from this result. The fortunate, but reliable error compensation observed frequently^[44, 69] for the cheapest method used here, namely B3LYP/6-31+G(d), is not perfect for chlorine nitrate species,

Table 1. Electronic energies in kcal mol⁻¹ for the decomposition of chlorine nitrate by n water molecules. The first lines correspond to the separated molecules, the second lines correspond to the $\text{ClONO}_2 \cdot (\text{H}_2\text{O})_n$ minima (set to 0.00 kcal mol⁻¹ by definition), the third lines correspond to the transition states to the concerted nucleophilic substitution/proton transfer reaction (TS), and the last lines correspond to the $\text{HNO}_3 \cdot \text{HOCl} \cdot (\text{H}_2\text{O})_{n-1}$ minima. CCSD(T) energies rely on MP2/aug-cc-pVDZ geometries. G2(MP2) values were calculated according to the literature,^[41] but without zero-point correction.

		B3LYP/ 6-31+G(d)	MP2/ aug-cc-pVDZ	CCSD(T)/ 6-31+G(d)	CCSD(T)/ aug-cc-pVDZ	G2(MP2)
$n=1$	$\text{ClONO}_2/\text{H}_2\text{O}$	5.24	3.76	4.80	–	–
	$\text{ClONO}_2 \cdot \text{H}_2\text{O}$	0.00	0.00	0.00	0.00	0.00
	TS	47.21	62.84	61.70	58.20	58.61
$n=2$	$\text{HNO}_3 \cdot \text{HOCl}$	–1.02	2.20	–0.23	–	–
	$\text{ClONO}_2/2\text{H}_2\text{O}$	15.60	–	–	–	–
	$\text{ClONO}_2 \cdot (\text{H}_2\text{O})_2$	0.00	0.00	0.00	0.00	0.00
	TS	22.37	25.89	29.80	26.47	26.63
$n=3$	$\text{HNO}_3 \cdot \text{HOCl} \cdot \text{H}_2\text{O}$	–5.77	–3.36	–4.55	–	–
	$\text{ClONO}_2/3\text{H}_2\text{O}$	27.59	–	–	–	–
	$\text{ClONO}_2 \cdot (\text{H}_2\text{O})_3$	0.00	0.00	0.00	–	0.00
	TS	14.96	18.83	23.00	–	19.95
	$\text{HNO}_3 \cdot \text{HOCl} \cdot (\text{H}_2\text{O})_2$	–0.52	–	–	–	–

but still good enough, so that it can be employed as reliable method for the huge amount of calculations along the reaction path and the subsequent interpolation procedure. We decided to use G2(MP2) as the “high level of theory” in the interpolation scheme as this method yields accurate reaction barriers and as we were able to compute the reaction barrier for all systems under investigation, that is, also for the system containing three water molecules. The reaction barrier to unimolecular isomerization in the latter system was found to be 20 kcal mol^{-1} . Introducing even more water molecules has been shown to diminish the reaction barrier even further so that a fast reaction is expected because of preferential solvation of the transition state.^[25–28, 67]

Reaction mechanism: From the mechanistic point of view the decomposition reaction is a nucleophilic substitution reaction coupled to a (multiple) proton transfer. The nucleophile is a water molecule attacking the electrophile chlorine. The accompanying proton transfer enhances the nucleophilicity of the attacking water molecule, as a species akin to the hydroxyl anion is generated. At the same time the basicity of the leaving group, the nitrate anion, is reduced because of the proton transfer. As the reaction coordinate involves a single transition state and no intermediates, a bimolecular reaction will result, and the correct nomenclature is S_N2 . In order to take the coupled proton transfer (PT) into consideration the nomenclature S_N2/PT is useful.

For an analysis of the reaction mechanism Figure 3 and Figure 4 can be used. First, the water and the chlorine nitrate molecules change their relative orientation by translational and rotational motions. Figure 3 shows that most reorienta-

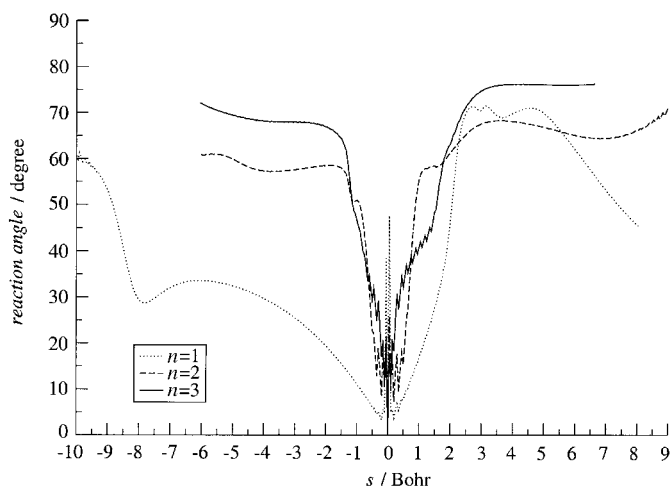


Figure 3. Angle between the reaction coordinate at the transition state, that is, normal-mode vector of the “imaginary” frequency, and the gradient along the reaction path. Negative s values correspond to $\text{ClONO}_2\text{-H}_2\text{O}$ species, $s = 0$ Bohr corresponds to the transition state, and positive s values correspond to HOCl-HNO_3 species.

tion is required for the $n = 1$ reaction, where the reaction angle changes from 60 to 30° . After the molecules have been arranged favourably the chemical reaction events begin, that is, bond-breaking and bond-making. The chlorine atom is transferred from O4 to O6 (for nomenclature cf. Figure 4).

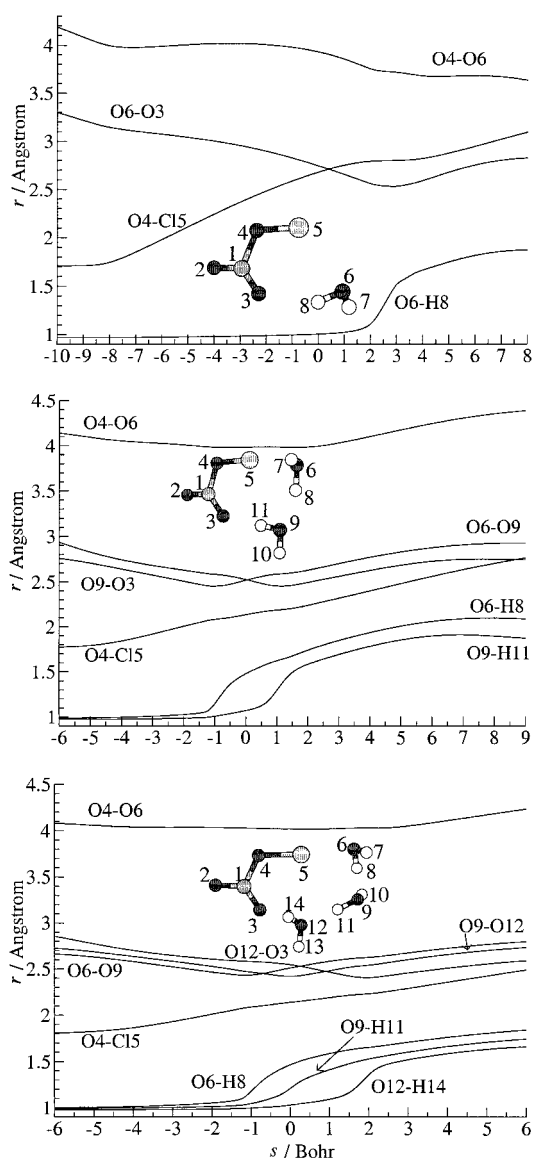


Figure 4. Distances r [in Å] between selected two atoms along the minimum energy path for the decomposition of chlorine nitrate by one (top), by two (middle) or by three (bottom) water molecules. The numbering scheme is shown as inset in the respective plots.

In contrast to proton transfer no minimum in the O4–O6 distance is required to trigger chlorine transfer. While the O4–Cl5 distance increases from 1.71 to 2.68 Å the proton to be transferred (H8) changes its distance to the water oxygen (O6) only from 0.97 to 1.00 Å ($n = 1$). In comparison to hydrogen atom transfer the reaction angle (cf. Figure 3) changes rather slowly in the case of chlorine atom transfer. This indicates that chlorine movement is less coupled to other vibrational degrees of freedom than hydrogen atom transfer. As the reaction coordinate motion at the transition state still corresponds to chlorine movement, “the imaginary frequency” is rather low, namely $172i \text{ cm}^{-1}$ ($n = 1$). The movement of the chlorine atom, which has a large van der Waals radius of 1.8 Å compared with 1.0 Å of the hydrogen atom, slowly compresses the O–O distances involved in hydrogen bonding. When the minimal O–O distance of 2.5 Å is reached the proton transfer of H8 is triggered. Namely, H8 increases the

distance to O6 to 1.87 Å, whereas the O4–Cl5 distance increases only by 0.41 Å ($n = 1$). This movement accelerates the compression of the neighbouring hydrogen bond (for $n = 2$ and $n = 3$). Again, at the minimal O–O distance of 2.5 Å the proton H11 is transferred. Obviously, the protons are not transferred at the same time, but in an asynchronous manner. For $n = 3$ H8 is transferred before the transition state, H11 at the transition state and the last proton transfer of H14 to the nitrate anion after having passed the transition state. When comparing the proton transfer locations with the potential energy in Figure 2, it becomes clear that the protons are transferred in regions where the gradient is rather high. The ionic structures do not correspond to minima, therefore, and the proton transfer events occur concertedly. The additional water molecules act both as a proton acceptor and proton donor and lower the reaction barrier, that is, they act as “bifunctional catalysts”. Also in the case of the decomposition of carbonic acid (H₂CO₃),^[70] the hydrations of sulfur dioxide^[71] and sulfur trioxide^[72] the water molecules have been shown to play this bifunctional role. Chlorine movement occurs at any stage of the reaction, that is, synchronously to the proton transfer reactions. In the transition state itself “the moving” proton is found at the position that shows the maximal distance both to the hydroxyl like nucleophile and the leaving group nitrate. This ensures that both a strong nucleophile and a good leaving group govern the reaction.

The influence of tunneling: The tunneling correction factors κ reflecting the reaction rate enhancement compared with the classical over-barrier reaction are depicted in Figure 5. For $n = 1$ tunneling plays only a marginal role due to the broad barrier caused by the movement of the chlorine atom. For $n = 2$ and $n = 3$ tunneling significantly influences the reaction rate only at temperatures $T < 175$ K. At these temperatures the dominant mechanism corresponds to a direct corner cutting through the reaction swath. The representative tunneling energy, at which the average molecule enters the classically forbidden tunneling region, is 0.1, 5, 7 and 10 kcal mol⁻¹ below the barrier top at 200 K, 175 K, 150 K and 100 K, respectively for $n = 2$. At approximately 175 K there is a jump in the representative tunneling energy indicating the crossover from the classically dominated regime to the quantum regime. This jump is also evident in Figure 5, where the tunneling correction significantly contributes to the reaction rate below 175 K. For $n = 3$ this sharp transition occurs at 125 K. The structures corresponding to the entrance into and exit out of the classically forbidden region at 100 K are depicted in Figure 6. It can be seen that both proton transfer reactions occur in the classically forbidden region. This is valid also at 175 K for $n = 2$. On the other hand at 200 K the most probable tunneling energy is very close to the barrier top, so that none of the two protons can tunnel. For $n = 3$ at temperatures above 125 K none of the protons tunnels, whereas at temperatures below 125 K all three protons tunnel through the reaction swath. No temperatures can be found, at which only one or two protons tunnel. Either all or none of the protons tunnel!

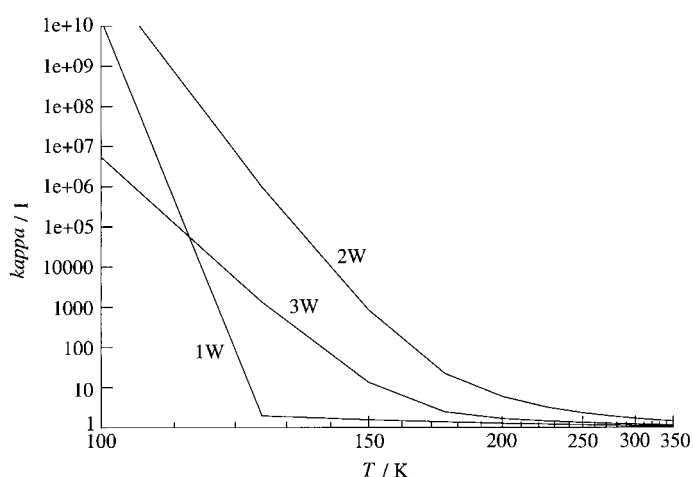


Figure 5. Tunneling correction factors κ for the decomposition of chlorine nitrate in a unimolecular complex containing one (“1W”), two (“2W”) or three (“3W”) water molecules as calculated at a B3LYP/6-31+G(d) potential energy surface and interpolated to G2(MP2) reaction barriers.

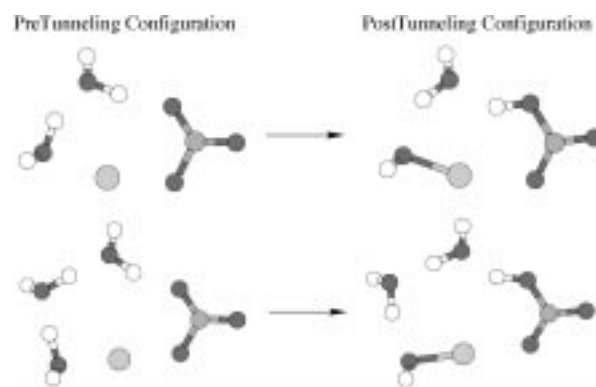


Figure 6. Representative minimum energy path configurations, at which the classical region on the potential energy surface is left (pre-tunneling configuration) and re-entered (post-tunneling configuration) at 100 K in the chlorine nitrate–two water (top) and chlorine nitrate–three water (bottom) system.

Rate constants: The main result of this study, summarized in Figure 7, is the extreme sensitivity of the reaction rate constant of chlorine nitrate hydrolysis on the amount of freely available water. This result is perfectly consistent with the experimental interpretation.^[18–23] In the case of the barrierless reaction in large water clusters the hydrolysis would supposedly even be collision limited. These rate constants explain why the reaction probabilities for Equation (1) decrease on increasing the acid concentration on the reaction surface. Namely, the reaction becomes slower, because there is less free water available for complexation. The rate constant of $3.9 \times 10^{-9} \text{ s}^{-1}$ at 200 K in the case of the three-water bridge is already close to the parameter of $1.0 \times 10^{-5} \text{ s}^{-1}$ used previously for reproducing past and predicting future ozone levels of the stratosphere.^[33] On the other hand both sets of rate constants involving just one and two water molecules are slower by more than 10 and 50 orders of magnitude, respectively. In our opinion, the best gas-phase model representing chlorine nitrate decomposition on an ice surface is therefore made up of one molecule of chlorine nitrate and three molecules of water. The fact that the first-

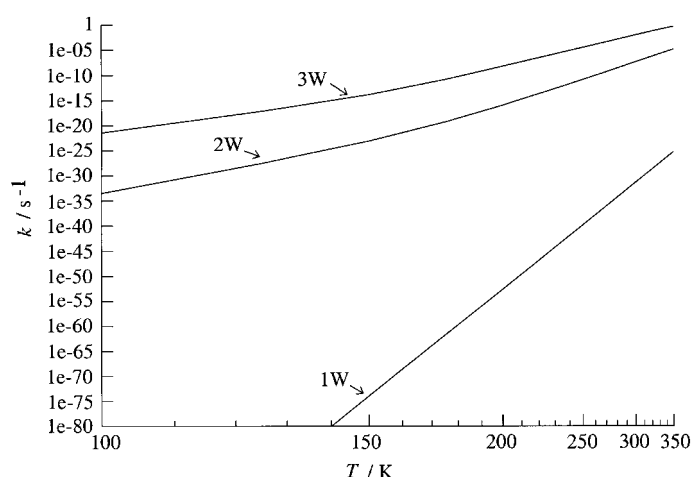


Figure 7. Reaction rate constants for the decomposition of chlorine nitrate in a unimolecular complex containing one (“1W”), two (“2W”) or three (“3W”) water molecules as calculated at a B3LYP/6-31+G(d) potential energy surface and interpolated to G2(MP2) reaction barriers. Note that the range of times reaches from seconds to days (10^{-5} s^{-1}) and years (10^{-10} s^{-1}) to many millions of years ($< 10^{-20} \text{ s}^{-1}$).

order rate coefficients for the decomposition of chlorine nitrate in a small gas-phase cluster and on an ice surface are very similar is a hint at a liquid-like nature of the surface. This has also been conjectured to be the case for PSCs from laboratory studies.^[13, 15, 73] Presumably the number of freely available water molecules per molecule of incoming ClONO_2 in PSCs is limited to about three. Interestingly, a recent uptake study of chlorine containing species on water clusters revealed a similar binding at a ratio of 1:3.^[74]

Conclusion

We presented a comparison of reaction rate constants for the hydrolysis of chlorine nitrate in the presence of one, two and three water molecules. We found that water acts as a bifunctional catalyst. Increasing the amount of water molecules dramatically accelerates the reaction. Tunneling does not play a decisive role in the model clusters at atmospheric temperatures. However, below 175 K for the 1:2 complex and below 125 K for the 1:3 complex multiple proton tunneling starts to be important and accelerates the reaction by several orders of magnitude. In these rather simple model systems the decomposition mechanism involves concerted, but asynchronous triple proton transfer as depicted in Figure 8. Tunneling favours such a concerted mechanism, as the highest tunneling probabilities are found when all protons tunnel in a single step. We could find no temperature at which a single proton tunnels for the 1:2 or 1:3 complexes. On the other hand experiments show that increasing the temperature and/or the

water availability favours a stepwise mechanism involving ions.^[27, 65, 66] In a very interesting study Horn, Sodeau, Roddis and Williams could detect a transition from the stepwise to the concerted regime by recording IR spectra first at 180 K and then lowering the temperature to 140 K.^[23] According to our results a possible explanation for this transition is the onset of concerted proton tunneling when the temperature is lowered below the crossover-temperature. It remains to be investigated whether incorporation of the confinement effects found on a true ice surface to our simple model cluster studied here (e.g. by adding microsolvating water molecules) leads to a quantitative agreement in terms of the crossover-temperature. Presently, the model system for which the first-order rate coefficient fits best with coefficients on ice surfaces is the 1:3 cluster as depicted in Figure 8 as determined in the laboratory. The rate constant found for this simple gas-phase model for the heterogeneous reaction on ice approximately reflects the one used in elaborate atmospheric modeling calculations on the ozone levels above Antarctica. In case that the simple model reaction would be used not as model for the heterogeneous reaction on an ice surface, but for the

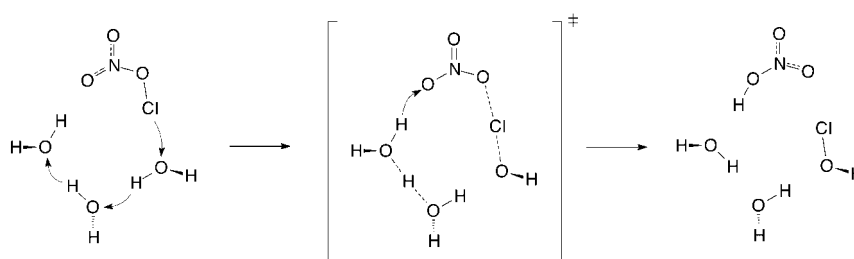


Figure 8. Model reaction mechanism for the hydrolysis of chlorine nitrate. The reaction path in the presence of three (and also two and one) water molecules undergoes only one transition state (“concerted $\text{S}_{\text{N}}2/\text{PT}$ reaction”) without any observable intermediate species. While the $\text{Cl}-\text{ONO}_2$ bond is elongated and a new $\text{HO}-\text{Cl}$ bond is formed, the three protons are transferred in compressed $\text{O}\cdots\text{H}-\text{O}$ hydrogen bonds one after the other (“asynchronously”).

homogeneous gas-phase reaction, the pre-association reaction to form the unimolecular complex had to be taken into account. While doing so and using a water concentration of 10^{14} molecules per cm^3 we arrived at a half-life for chlorine nitrate of many thousand years. This very slow reaction is consistent with the measurements done 20 years ago. Furtheron it shows that the observed ozone depletion above mid-latitudes is not due to homogeneous gas-phase chemistry, but rather a result of heterogeneous reactions on aerosols, particularly after volcanic eruptions.^[8]

Acknowledgement

T.L. is grateful to the Austrian Academy of Sciences for financial support. This study was supported by the Austrian Science Fund (project number P14357-TPH).

- [1] J. C. Farman, B. G. Gardiner, J. D. Shanklin, *Nature* **1985**, 315, 207–210.
- [2] S. Solomon, *Nature* **1990**, 347, 347–354.
- [3] P. O. Wennberg, R. C. Cohen, R. M. Stimpfle, J. P. Koplrow, J. G. Anderson, R. J. Salawitch, D. W. Fahey, E. L. Woodbridge, E. R. Keim, R. S. Gao, C. R. Webster, R. D. May, D. W. Toohey, L. M.

- Avallone, M. H. Proffitt, M. Loewenstein, J. R. Podolske, K. R. Chan, S. C. Wofsy, *Science* **1994**, *266*, 398–404.
- [4] P. J. Crutzen, J.-U. Groob, C. Brühl, R. Müller, J. M. Russell III, *Science* **1995**, *268*, 705–708.
- [5] K. S. Carslaw, M. Wirth, A. Tsias, B. P. Luo, A. Dörnbrack, M. Leutbecher, H. Volkert, W. Renger, J. T. Bacmeister, E. Reimer, T. Peter, *Nature* **1998**, *391*, 675–678.
- [6] D. W. Fahey, A. R. Ravishankara, *Science* **1999**, *285*, 208–210.
- [7] W. J. Randel, R. S. Stolarski, D. M. Cunnold, J. A. Logan, M. J. Newchurch, J. M. Zawodny, *Science* **1999**, *285*, 1689–1692.
- [8] S. Solomon, *Rev. Geophys.* **1999**, *37*, 275–316.
- [9] M. J. Molina, R. Zhang, P. J. Wooldridge, J. R. McMahon, J. E. Kim, H. Y. Chang, K. D. Beyer, *Science* **1993**, *261*, 1418–1423.
- [10] M. A. Tolbert, *Science* **1994**, *264*, 527–528.
- [11] S. Solomon, R. R. Garcia, F. S. Rowland, D. J. Wuebbles, *Nature* **1986**, *321*, 755–758.
- [12] P. J. Crutzen, F. Arnold, *Nature* **1986**, *324*, 651–655.
- [13] M. J. Molina, T.-L. Tso, L. T. Molina, F. C.-Y. Wang, *Science* **1987**, *238*, 1253–1257.
- [14] M. A. Tolbert, M. J. Rossi, R. Malhotra, D. M. Golden, *Science* **1987**, *238*, 1258–1260.
- [15] O. B. Toon, M. A. Tolbert, *Nature* **1995**, *375*, 218–221.
- [16] T. Koop, K. S. Carslaw, *Science* **1996**, *272*, 1638–1641.
- [17] J. Schreiner, C. Voigt, A. Kohlmann, F. Arnold, K. Mauersberger, N. Larsen, *Science* **1999**, *283*, 968–970.
- [18] D. R. Hanson, A. R. Ravishankara, *J. Phys. Chem.* **1992**, *96*, 2682–2691.
- [19] J. P. D. Abbatt, M. J. Molina, *J. Phys. Chem.* **1992**, *96*, 7674–7679.
- [20] R. Oppliger, A. Allan, M. J. Rossi, *J. Phys. Chem. A* **1997**, *101*, 1903–1911.
- [21] S. B. Barone, M. A. Zondlo, M. A. Tolbert, *J. Phys. Chem. A* **1997**, *101*, 8643–8652.
- [22] B. S. Berland, M. A. Tolbert, S. M. George, *J. Phys. Chem. A* **1997**, *101*, 9954–9963.
- [23] A. B. Horn, J. R. Sodeau, T. B. Roddis, N. A. Williams, *J. Chem. Soc. Faraday Trans.* **1998**, *94*, 1721–1724.
- [24] L. Ying, X. Zhao, *J. Phys. Chem. A* **1997**, *101*, 6807–6812.
- [25] R. Bianco, J. T. Hynes, *J. Phys. Chem. A* **1998**, *102*, 309–314.
- [26] R. Bianco, B. J. Gertner, J. T. Hynes, *Ber. Bunsen.-Ges. Phys. Chem.* **1998**, *102*, 518–526.
- [27] J. P. McNamara, I. H. Hillier, *J. Phys. Chem. A* **1999**, *103*, 7310–7321.
- [28] J. P. McNamara, G. Tresadern, I. H. Hillier, *Chem. Phys. Lett.* **1999**, *310*, 265–270.
- [29] S. C. Xu, X. S. Zhao, *J. Phys. Chem. A* **1999**, *103*, 2100–2106.
- [30] D. R. Hanson, *J. Phys. Chem.* **1995**, *99*, 13059–13061.
- [31] A. B. Horn, J. R. Sodeau, T. B. Roddis, N. A. Williams, *J. Phys. Chem. A* **1998**, *102*, 6107–6120.
- [32] H. A. Donsig, D. Herridge, J. C. Vickerman, *J. Phys. Chem. A* **1999**, *103*, 9211–9220.
- [33] M. B. McElroy, R. J. Salawitch, S. C. Wofsy, J. A. Logan, *Nature* **1986**, *321*, 759–762.
- [34] T. Loerting, K. R. Liedl, unpublished results.
- [35] A. D. Becke, *J. Chem. Phys.* **1993**, *98*, 5648–5652.
- [36] P. J. Stephens, F. J. Devlin, C. F. Chabalowski, M. J. Frisch, *J. Phys. Chem.* **1994**, *98*, 11623–11627.
- [37] C. Møller, M. S. Plesset, *Phys. Rev.* **1934**, *46*, 618–622.
- [38] *Gaussian 98*, Revision A.7, Gaussian, Inc. Pittsburgh, PA, **1998**.
- [39] T. Loerting, K. R. Liedl, *J. Phys. Chem. A* **1999**, *103*, 9022–9028.
- [40] K. Raghavachari, G. W. Trucks, J. A. Pople, M. Head-Gordon, *Chem. Phys. Lett.* **1989**, *157*, 479–483.
- [41] L. A. Curtiss, K. Raghavachari, J. A. Pople, *J. Chem. Phys.* **1993**, *98*, 1293–1298.
- [42] M. Page, J. W. McIver, Jr., *J. Chem. Phys.* **1988**, *88*, 922–935.
- [43] T. Loerting, K. R. Liedl, B. M. Rode, *J. Am. Chem. Soc.* **1998**, *120*, 404–412.
- [44] T. Loerting, K. R. Liedl, B. M. Rode, *J. Chem. Phys.* **1998**, *109*, 2672–2679.
- [45] T. Loerting, K. R. Liedl, *J. Am. Chem. Soc.* **1998**, *120*, 12595–12600.
- [46] H. Eyring, *J. Chem. Phys.* **1935**, *3*, 107–115.
- [47] D. G. Truhlar, B. C. Garrett, *Ann. Rev. Phys. Chem.* **1984**, *35*, 159–189.
- [48] *Polyrate 8.2*, University of Minnesota, Minneapolis, **1999**.
- [49] *Gaussrate 8.2*, University of Minnesota, Minneapolis, **1999**.
- [50] W.-P. Hu, Y.-P. Liu, D. G. Truhlar, *J. Chem. Soc. Faraday Trans.* **1994**, *90*, 1715–1725.
- [51] J. C. Corchado, J. Espinosa-Garcia, W.-P. Hu, I. Rossi, D. G. Truhlar, *J. Phys. Chem.* **1995**, *99*, 687–694.
- [52] K. A. Nguyen, I. Rossi, D. G. Truhlar, *J. Chem. Phys.* **1995**, *103*, 5522–5530.
- [53] Y.-Y. Chuang, D. G. Truhlar, *J. Phys. Chem. A* **1997**, *101*, 3808–3814.
- [54] “Generalized Transition State Theory” D. G. Truhlar, A. D. Isaacson, B. C. Garrett in *Theory of Chemical Reaction Dynamics* (Ed.: M. Baer), CRC, Boca Raton, FL, **1985**, pp. 65–137.
- [55] “Transition State Theory” M. M. Kreevoy, D. G. Truhlar in *Investigation of Rates and Mechanisms of Reactions* (Ed.: C. F. Bernasconi), Wiley, New York, **1986**, pp. 13–95.
- [56] “Dynamical Formulation of Transition State Theory: Variational Transition States and Semiclassical Tunneling” S. C. Tucker, D. G. Truhlar, *New Theoretical Concepts for Understanding Organic Reactions* (Eds.: J. Bertrán, I. G. Csizmadia), Kluwer, Dordrecht, The Netherlands, *NATO ASI Ser. C* **1989**, *267*, pp. 291–346.
- [57] D. G. Truhlar, M. S. Gordon, *Science* **1990**, *249*, 491–498.
- [58] R. T. Skodje, D. G. Truhlar, B. C. Garrett, *J. Phys. Chem.* **1981**, *85*, 3019–3023.
- [59] K. K. Baldrige, M. S. Gordon, R. Steckler, D. G. Truhlar, *J. Phys. Chem.* **1989**, *93*, 5107–5119.
- [60] B. C. Garrett, D. G. Truhlar, *J. Chem. Phys.* **1983**, *79*, 4931–4938.
- [61] G. C. Lynch, D. G. Truhlar, B. C. Garrett, *J. Chem. Phys.* **1989**, *90*, 3102–3109.
- [62] B. C. Garrett, T. Joseph, T. N. Truong, D. G. Truhlar, *Chem. Phys.* **1989**, *136*, 271–283.
- [63] Y.-P. Liu, D.-H. Lu, A. Gonzalez-Lafont, D. G. Truhlar, B. C. Garrett, *J. Am. Chem. Soc.* **1993**, *115*, 7806–7817.
- [64] A. Fernández-Ramos, D. G. Truhlar, *J. Chem. Phys.* **2001**, *114*, 1491–1496.
- [65] S. F. Banham, A. B. Horn, T. G. Koch, J. R. Sodeau, *Farad. Disc. Chem. Soc.* **1995**, *100*, 321–332.
- [66] J. R. Sodeau, A. B. Horn, S. F. Banham, T. G. Koch, *J. Phys. Chem.* **1995**, *99*, 6258–6262.
- [67] E. V. Akhmatkaya, C. J. Apps, I. H. Hillier, A. J. Masters, I. J. Palmer, N. E. Watt, M. A. Vincent, J. C. Whitehead, *J. Chem. Soc. Faraday Trans.* **1997**, *93*, 2775–2779.
- [68] B. J. Lynch, P. L. Fast, M. Harris, D. G. Truhlar, *J. Phys. Chem. A* **2000**, *104*, 4811–4815.
- [69] C. Märker, P. v. R. Schleyer, K. R. Liedl, T.-K. Ha, M. Quack, M. A. Suhm, *J. Comput. Chem.* **1997**, *18*, 1695–1719.
- [70] T. Loerting, C. Tautermann, R. T. Kroemer, I. Kohl, A. Hallbrucker, E. Mayer, K. R. Liedl, *Angew. Chem.* **2000**, *112*, 919–922; *Angew. Chem. Int. Ed.* **2000**, *39*, 891–894.
- [71] T. Loerting, R. T. Kroemer, K. R. Liedl, *Chem. Commun.* **2000**, 999–1000.
- [72] T. Loerting, K. R. Liedl, *Proc. Natl. Acad. Sci. USA* **2000**, *97*, 8874–8878.
- [73] S.-H. Lee, D. C. Leard, R. Zhang, L. T. Molina, M. J. Molina, *Chem. Phys. Lett.* **1999**, *315*, 7–11.
- [74] R. S. MacTaylor, J. J. Gilligan, D. J. Moody, A. W. Castleman, Jr., *J. Phys. Chem. A* **1999**, *103*, 4196–4201.

Received: September 20, 2000 [F2737]